

SHORT COMMUNICATION

Current distribution in a gas-evolving electrochemical reactor with an expanded metal electrode

J. M. BISANG

Programa de Electroquímica Aplicada e Ingeniería Electroquímica (PRELINE), Facultad de Ingeniería Química, Universidad Nacional del Litoral, Santiago del Estero 2829, 3000 Santa Fe, Argentina

Received 1 July 1991; revised 29 August 1991

Nomenclature

b	constant in the Tafel equation = $\alpha v_e F/RT$ (V^{-1})
e	electrode thickness (cm)
F	Faraday constant ($A s mol^{-1}$)
i	current density ($A cm^{-2}$)
I	total current (A)
L	electrode length (cm)
N_{Mac}	MacMullin number
Q	volumetric liquid flow rate ($cm^3 s^{-1}$)
R	gas constant ($JK^{-1} mol^{-1}$)
S_i	i th electrode-to-membrane gap (cm)
S_D	separator thickness (cm)
T	temperature (K)
v_s	single bubble rise velocity ($cm s^{-1}$)
W	electrode width (cm)
y	axial coordinate (cm)

Greek characters

α	charge transfer coefficient
$\bar{\delta}_r$	mean relative deviation
ε_m	limiting gas voidage
v_e	charge number of the electrode reaction
ρ_0	electrolyte resistivity (Ωcm)
ρ_m	metal phase resistivity (Ωcm)
$\rho_{m,ef}$	effective resistivity of the expanded structure (Ωcm)

Subscript

a	anodic
b	cathodic

1. Introduction

During the last few years expanded metal structures have received considerable attention for possible applications in the field of applied electrochemistry. The expanded metal structure presents a specific surface area larger than that for planar electrodes and it also promotes turbulence. Expanded metal electrodes may therefore be used as efficient electrodes for electrochemical reactions with mass-transfer control, such as the removal of heavy metals from dilute solutions [1]. Thus some authors have investigated the mass transfer conditions to the electrode surface [2–8] and the current distribution in stacks of sheets of expanded metal [4, 5].

Similarly, in the case of gas-evolving electrochemical reactions expanded metal electrodes are also efficient since they can be orientated to promote the exit of gas bubbles from the interelectrode gap, thus decreasing the ohmic potential drop in the solution phase [9, 10].

However expanded metals have a void fraction and a tortuosity factor, which lead to a current distribution more uneven than that for a planar electrode under the same conditions.

The aim of this work is to determine experimentally the current distribution in a gas-evolving electrochemical reactor with an expanded electrode and to compare the experimental results with the theoretical

current distribution predicted by the mathematical model reported in previous work [11].

2. Experimental details

The determination of current distribution was performed in an electrochemical reactor with parallel plate electrodes employing a segmented cathode. The reactor was made of acrylic material and both electrodes had the same dimensions, 200 mm wide and 600 mm long.

The nickel cathode was made of 192 squares, 24 mm side and 1 mm thick, arranged in 8 columns of 24 elements. The anode was a sheet of expanded titanium coated with RuO_2 (DSA). Figure 1 shows the dimensions of the anode. The void fraction and the tortuosity factor of the expanded metal were 0.5 and 1.1, respectively, thus the effective resistivity of the anode was 2.2 times the value of the titanium resistivity. The anode was electrically fed along its lower edge and was placed with the large diagonal parallel to the solution flow direction.

The anodic and cathodic compartments were separated by a diaphragm of asbestos cloth 2 mm thick and the electrode-to-separator gaps were 13 mm. The temperature was approximately 30°C.

Further details of the equipment employed, method of operation, data acquisition, test reactions and reagents can be obtained from previous work [11].

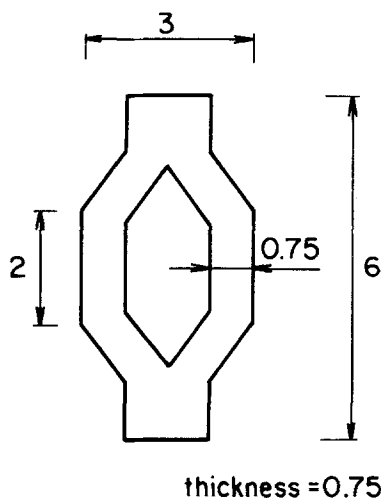


Fig. 1. Characteristic parameters of the expanded structure. Dimensions in millimetres.

3. Results and discussion

Figures 2 and 3 show the current density as a function of position for several values of the total current. Each point is the mean value of the current density of the eight columns for a given value of y and the relative error, with respect to the mean value, is approximately $\pm 10\%$.

The full lines represent the current distribution according to the previously reported model [11], which is based in a voltage balance at each axial position in the reactor taking into account the overpotentials at both electrodes and the ohmic drops in the metal phase of the anode, in the anodic and cathodic compartments and in the diaphragm. The ohmic drop in the metal phase of the cathode was neglected due to the special construction of the reactor used in this work. To calculate the gas voidage the Kreysa and Kuhn coalescence barrier model [12] was used combined with the Richardson-Zaki equation to describe the motion of the bubbles. The effective resistivity of the gas-electrolyte dispersions was calculated by the Bruggeman equation. The ohmic drop across the catalytic oxide layer of the anode was neglected.

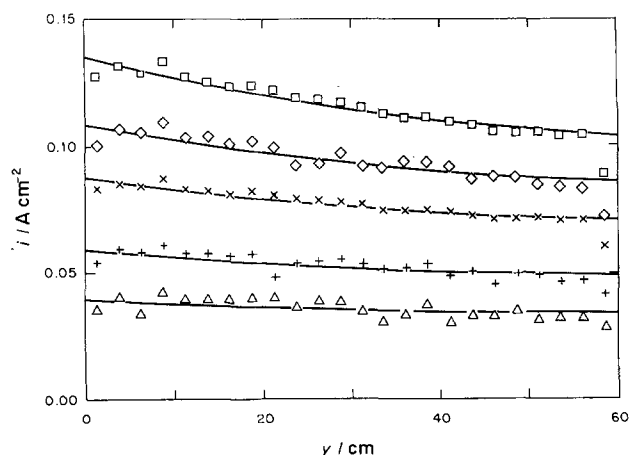


Fig. 2. Experimental and theoretical (—) [11] current distributions at different total currents. (Δ) 42.93, (+) 63.14, (x) 92.76, (\diamond) 113.50, (\square) 139.24 A. Parameters according to Table 1.

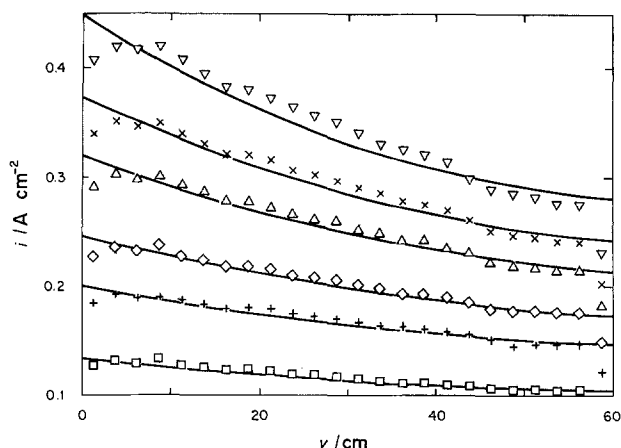


Fig. 3. Experimental and theoretical (—) [11] current distributions at different total currents. (\square) 139.24, (+) 201.40, (\diamond) 242.75, (Δ) 306.21, (x) 350.81, (∇) 411.06 A. Parameters according to Table 1.

The parameters used in the calculations are summarized in Table 1. The agreement between the calculated and the measured current distributions is denoted by the mean relative deviation, which is given in Table 2.

From Figs 2 and 3 and Table 2 it can be seen that the agreement between the theoretical and experimental results is close and therefore the suitability of the model to design gas-evolving electrochemical reactors is confirmed.

In Fig. 4 the influence of the anodic metal phase on the current distribution is analysed, for which the mathematical model [11] was solved for different values of the metal resistivity of the anode. The curves a are the same as those of Fig. 3 and were obtained taking into account the effective resistivity of the expanded structure. The curves b represent the current distribution of a gas-evolving electrochemical reactor with a planar RuO_2 -coated titanium anode; the curves c were obtained by neglecting the ohmic drop term of the metal phase in the voltage balance equation, thus only the overpotentials and the ohmic drops in both compartments and diaphragm were considered. Therefore, the comparison between the curves a and b yields the effect of the expanded structure on the current distribution. The comparison between a or b with c curves gives the effect of the anodic metal phase.

It can be observed that, for this electrochemical reactor, the effective resistivity of the expanded struc-

Table 1. Summary of the parameters used in modelling

ρ^0	5.56 Ω cm	L	60 cm
$\varepsilon_{m,a}$	0.26	W	20 cm
$\varepsilon_{m,c}$	0.38	e	0.075 cm
$v_{s,a}$	4.5 cm s^{-1}	S_a	1.3 cm
$v_{s,c}$	3.5 cm s^{-1}	S_c	1.3 cm
Q	112 $\text{cm}^3 \text{s}^{-1}$	S_D	0.2 cm
Q_a	0.5 Q	b_a	38.38 V^{-1}
Q_c	0.5 Q	b_c	25.58 V^{-1}
ρ_m	$4.95 \times 10^{-5} \Omega$ cm	$v_{e,a}$	4
$\rho_{m,ef}$	$1.09 \times 10^{-4} \Omega$ cm	$v_{e,c}$	2
N_{mac}	2		

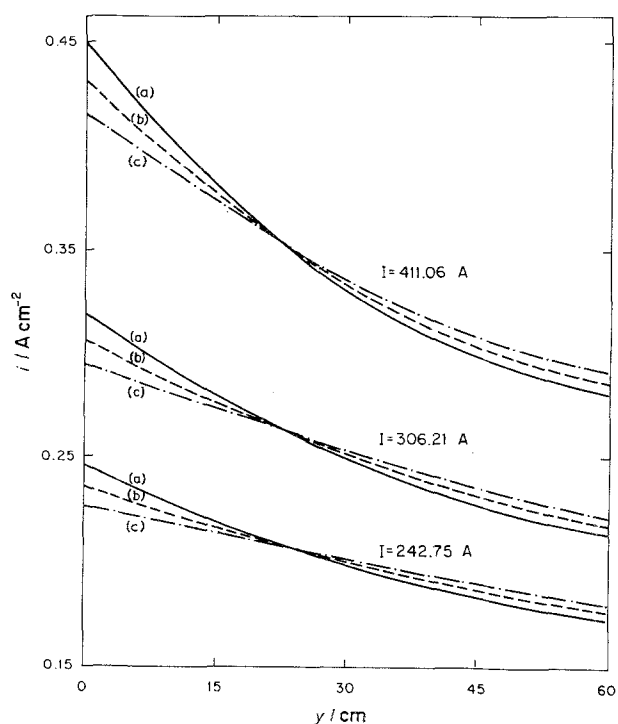


Fig. 4. Effect of the metal phase resistivity on the current distribution. The calculations were made with the mathematical model reported in [11]. (a) expanded titanium anode ($\rho_{m,er} = 1.09 \times 10^{-4} \Omega \text{ cm}$), (b) planar RuO_2 -coated titanium ($\rho_m = 4.95 \times 10^{-5} \Omega \text{ cm}$), (c) $\rho_m = 0$. Other parameters according to Table 1.

ture increases the non-uniformity in the current distribution notably even for low total currents. This deleterious effect of the expanded structure decreases the effectiveness factor of the electrode and must be taken into account in the design of electrochemical reactors.

Table 2. Review of the results

Fig. No.	Symbol	I/A	$\bar{\delta}_r \times 10^2$
2	Δ	42.93	7.41
2	+	63.14	4.84
2	x	92.76	2.10
2	\diamond	113.50	3.23
2 and 3	\square	139.24	2.02
3	+	201.40	2.73
3	\diamond	242.75	2.31
3	Δ	306.21	2.60
3	x	350.81	3.14
3	∇	411.06	3.86

References

- [1] P. M. Robertson, B. Scholder, G. Theis and N. Ibl, *Chem. Ind.* (1978) 459.
- [2] F. Leroux and F. Coeuret, *Electrochim. Acta* **28** (1983) 1857.
- [3] F. Coeuret and J. Legrand, *J. Appl. Electrochem.* **15** (1985) 181.
- [4] F. Leroux and F. Coeuret, *Electrochim. Acta* **30** (1985) 159.
- [5] *Idem, ibid.* **30** (1985) 167.
- [6] S. Piovano and U. Böhm, *J. Appl. Electrochem.* **17** (1987) 123.
- [7] *Idem, ibid.* **17** (1987) 127.
- [8] *Idem, ibid.* **19** (1989) 940.
- [9] G. Kreysa and H.-J. Kùlps, *J. Electrochem. Soc.* **128** (1981) 979.
- [10] C. Elsner and F. Coeuret, *J. Appl. Electrochem.* **15** (1985) 567.
- [11] J. M. Bisang, *ibid.* **21** (1991) 760.
- [12] G. Kreysa and M. Kuhn, *ibid.* **15** (1985) 517.